

Topological feature and phase structure of QCD at complex chemical potential[☆]

Kouji Kashiwa^a, Akira Ohnishi^a

^a*Yukawa Institute for Theoretical Physics, Kyoto University, Kyoto 606-8502, Japan*

Abstract

The pseudo-critical temperature of the confinement-deconfinement transition and the phase transition surface are investigated by using the complex chemical potential. We can interpret the imaginary chemical potential as the Aharonov-Bohm phase, then the analogy of the topological order suggests that the Roberge-Weiss endpoint would define the pseudo-critical temperature. The behavior of the Roberge-Weiss endpoint at small real quark chemical potential is investigated with the perturbative expansion. The expected QCD phase diagram at complex chemical potential is presented.

Keywords: QCD phase diagram, Deconfinement transition, Complex chemical potential

1. Introduction

Understanding the phase structure of Quantum Chromodynamics (QCD) is one of the most important and interesting subjects in nuclear and elementary particle physics. The lattice QCD simulation is a powerful and gauge invariant method, but it has the sign problem at finite real chemical potential (μ_R), and we cannot obtain reliable results at large μ_R . Some methods are proposed to circumvent the sign problem, see Ref. [1] as an example, but those methods are limited in the $\mu_R/T < 1$ region where T is temperature. Because of the sign problem, low energy effective models of QCD are extensively used to explore the QCD phase structure. Effective models, however, have strong ambiguities and thus quantitative predictions are impossible at present. Towards unification of lattice QCD simulations and effective model approaches, a new method so-called *imaginary chemical potential matching approach* [2, 3] is proposed recently. In this method, we use lattice QCD data obtained at finite imaginary chemical potential (μ_I) to constrain effective models. It is well known that the sign problem does not exist in the finite μ_I region and the region has information on the μ_R region; constrained models are reliable not only at finite μ_I but also at finite μ_R .

In addition to the imaginary chemical potential matching approach, the concept of the imaginary chemical potential may be important to define the confinement-deconfinement transition. In the imaginary time formalism where its time direction is compactified, the imaginary chemical potential can be interpreted as the Aharonov-Bohm phase induced by $U(1)$ flux insertions to the closed time loop. From this interpretation, we can determine the pseudo-critical temperature of the deconfinement transition from the Roberge-Weiss (RW) endpoint [4] with an analogy of the topological order [5, 6] as explained later.

It is also interesting to investigate the phase structure at *finite complex* chemical potential, $\mu = \mu_R + i\mu_I$, where $\mu_R \neq 0$ and

$\mu_I \neq 0$. On the (T, μ_R) plane ($\mu_I = 0$), the first order phase transition may exist, then we would have the critical point (CP) as the endpoint of the first order phase transition boundary. On the (T, μ_I) plane ($\mu_R = 0$), the first order RW transition line exists, and the RW endpoint can either be the first or the second order. Some lattice QCD simulations [7, 8, 9] suggest that the order of the RW endpoint is the first order at the physical pion mass. Then the RW endpoint is a triple point, with two other first order lines departing from the RW transition line. The first order lines appear around the heavy quark limit as well as around the chiral limit [7, 9]. These lines with small quark mass may have the chiral transition nature and are referred to as the *chiral critical* lines. One of the chiral critical lines extending in the $\mu_I \rightarrow 0$ direction should have an endpoint (chiral critical endpoint; CCE) before reaching the $\mu_I = 0$ plane as long as the $\mu = 0$ transition is crossover. Figure 1 summarizes our current expectation of the QCD phase diagram. Now we can raise a question. How does CCE behave at complex chemical potential? Specifically, is CCE on the (T, μ_I) plane connected with CP on the (T, μ_R) plane at complex chemical potential, *i.e.* in the (T, μ_R, μ_I) space? The topology of the phase diagram at complex chemical potential would tell us the relation between the deconfinement and the chiral transition.

In this letter, first we briefly summarize properties of QCD at finite imaginary chemical potential, and propose a new definition of the pseudo-critical temperature of the deconfinement transition by the RW endpoint temperature (T_{RW}). Next, we investigate the behavior of the RW endpoint at small μ_R by using the perturbative expansion. Finally, we present two scenarios of the QCD phase diagram at complex chemical potential based on the behavior of the RW endpoint at small μ_R and a symmetry argument.

2. QCD with imaginary chemical potential

At finite μ_I , QCD has a special periodicity so-called the RW periodicity [4]. The RW periodicity can cause the first order

[☆]Report number: YITP-15-45

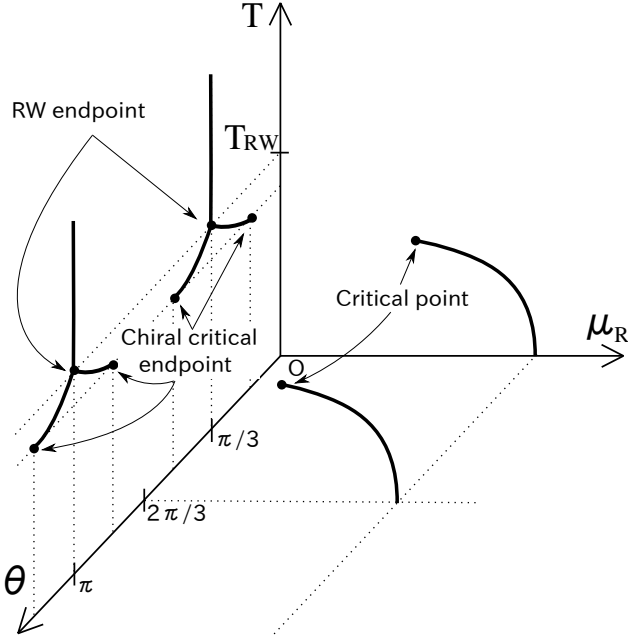


Figure 1: Schematic figure of our current expectation of the QCD phase diagram at finite μ_R and μ_I , respectively. Solid lines represent the first order transition line.

transition lines (RW transition lines) and their endpoints (RW endpoints). Those are predicted by using the strong coupling QCD and the perturbative one-loop effective potential approach with a background gauge field. The RW periodicity can be seen from the relation of the grand-canonical partition function Z [4]:

$$Z(\theta) = Z\left(\theta + \frac{2\pi k}{3}\right), \quad (1)$$

where a dimensionless quark chemical potential is defined as $\theta \equiv \mu_I/T \in \mathbb{R}$ and k is any integer. If quarks are confined, physical states are classified by hadron degrees of freedom unlike the deconfined phase. In the confined and deconfined phases, origins of the RW periodicity are different:

Confined phase — The origin is the dimensionless baryon chemical potential 3θ in the form of $\exp(\pm 3i\theta)$ in the partition function. It can be easily seen, for example, from the strong coupling limit of the lattice QCD with the mean-field approximation [10, 11], the chiral perturbation theory with the relativistic Virial expansion [12] and that with the finite energy sum rule [13].

Deconfined phase — The origin is the quark chemical potential and the gauge field in the form of $\exp[\pm i(gA_4/T + \theta)]$. It generates color non-singlet contributions in the partition function. It can be understood from the perturbative one-loop effective potential with the background gauge field [14, 15], and the RW periodicity is then induced by \mathbb{Z}_3 images [4].

The first order RW transition lines at $\theta = \pi(2k + 1)/3$ are induced by \mathbb{Z}_3 images. Its endpoint which is nothing but the RW

endpoint should exist. The order of the RW endpoint is still under debate, but some lattice QCD simulations [7, 8, 9] suggest that the order seems to be first order around the physical pion mass.

3. Imaginary chemical potential and Aharonov-Bohm phase

In the imaginary time formalism where the temporal direction is compactified, the $U(1)$ flux can be inserted to the fictitious hole. Then, the imaginary chemical potential can be regarded as the Aharonov-Bohm phase [16]. In this interpretation, we may use the discussion of the topological order [5]. Actual applications to zero temperature QCD was discussed in Ref. [6].

In Ref. [6], the authors consider the torus T^3 at zero temperature, and introduce three adiabatic operations: (a) Insert the $U(1)$ flux to holes of spatial closed loops, (b) exchange i -th and $i + 1$ -th quarks and (c) move a quark along loops. Commutation relations of the operation (b) and (c) are described by the Braid group, and the Aharonov-Bohm effect determines the commutation relations of those with (a). If quarks are deconfined, operations become non-commutable because of the quark's fractional charge. It is commutable if quarks are confined because physical states are described by hadron degrees of freedom with integer charges. Therefore, if there is only one vacuum in the deconfined phase, it is inconsistent with the non-commutability of the operations and thus vacuum degeneracy should exist.

We here consider the $U(1)$ flux insertion of $2\pi/N_c$ to the fictitious hole at zero μ_I . This corresponds to change the $U(1)$ flux from $-\pi/N_c$ to π/N_c at $\theta = \pi/N_c$. These two states are free energy minima at $\theta = \pi/N_c$ and degenerated at $T > T_{RW}$, while they belong to the same minimum at $T < T_{RW}$. Thus the gluon configurations in states at $\theta = \pi/N_c$ are essentially the same as those at $\theta = 0$. In thermal equilibrium, the topological order cannot be well defined because thermal states are constructed by a superposition of pure states with the Boltzmann factor. Therefore, we cannot operate (a), (b) and (c), adiabatically. However, the RW periodicity shows significantly different behaviors in the confined and deconfined phases as already mentioned, and it is induced by the nontrivial appearance of the RW periodicity in the deconfined phase. This fact suggests that we can distinguish the confinement and deconfinement phases at $\mu_I = 0$ from the non-trivial degeneracy of the effective potential at $\theta = \pi/N_c$. This degeneracy seems similar to the vacuum degeneracy in zero T systems and the analogy can be found. Therefore, we propose that T_{RW} is the pseudo-critical temperature of the deconfinement transition. It should be noted that the present definition and the standard definition determined by using the Polyakov-loop are consistent in the pure gauge limit where the Polyakov-loop is the exact order-parameter of the deconfinement transition.

4. Roberge-Weiss endpoint at complex chemical potential

We now discuss the μ_R -dependence of the pseudo-critical temperature of the deconfinement defined by T_{RW} . We here

give an argument based on the perturbative expansion of the effective potential in μ_R as a first step to investigate the μ_R -dependence of the RW endpoint. It should be noted that non-perturbative model approaches have several difficulties. One of the promising effective models is the Polyakov-loop extended Nambu–Jona-Lasinio (PNJL) model [17]. The PNJL model has the model sign problem at finite μ_R [18]. There are some proposals to circumvent the model sign problem, for example the complex integral path contour [19, 20, 21] based on the Lefschetz thimble [22, 23, 24] and the complex Langevin dynamics [25, 26]. Unfortunately those approaches can not be directly used at finite complex chemical potential because we can not maintain the RW periodicity and some other desirable properties of QCD.

The effective potential at small μ_R are expanded to μ_R^2 order as

$$\begin{aligned} \mathcal{V}(T, \mu_R, \mu_I) &= \mathcal{V}(T, 0, \mu_I) - \left(\frac{\mu_R}{T}\right) (T n_q(\mu_R, \mu_I)|_{\mu_R=0}) \\ &\quad - \frac{1}{2} \left(\frac{\mu_R}{T}\right)^2 \frac{d[T n_q(\mu_R, \mu_I)]}{d\mu_R/T} \Big|_{\mu_R=0} + \mathcal{O}((\mu_R/T)^3) \end{aligned} \quad (2)$$

where

$$T \frac{dn_q}{d\mu_R/T} \Big|_{\mu_R=0} = T \frac{dn_q}{d(i\mu_I/T)} \Big|_{\mu_R=0} = -iT \frac{dn_q}{d\theta} \Big|_{\mu_R=0}. \quad (3)$$

Equation (3) is real, and the second term in r.h.s. of Eq. (2) should be pure imaginary.

We here neglect the imaginary part of the effective potential. This assumption corresponds to the phase quenched approximation. If the RW endpoint is the weak first order, the n_q gap at T_{RW} is small and the sign problem is mild, then the phase quenched approximation is justified. If the RW endpoint is the strong first order, the partition function at given (T, μ) is dominated by one classical vacuum, then the role of the imaginary part, or the phase of the state, is minor. The phase quenched approximation cannot be applied to the second order RW endpoint. Fortunately, the RW endpoint with the realistic quark mass is predicted to be the first order by lattice QCD simulations [7, 8, 9] and it would be possible to ignore the imaginary part of the effective potential. Effects of the imaginary part of the effective potential will be discussed elsewhere.

Next, we consider two set of solutions for the chiral order-parameter σ , the Polyakov-loop Φ and its conjugate $\bar{\Phi}$ which can be obtained by the minimization of $\text{Re } \mathcal{V}$ at $\mu_R = 0$ and $\theta = \pi/3$. We call the solution at $(T_{RW} - \epsilon)$ *confinement solution* which is labeled as $C_{-\epsilon}$ where ϵ is the infinitesimal value. Also, we call the solution at $(T_{RW} + \epsilon)$ *deconfinement solution* which is labeled as $C_{+\epsilon}$.

By comparing $\text{Re } \mathcal{V}$ with $C_{-\epsilon}$ to that with $C_{+\epsilon}$ in the $\epsilon \rightarrow 0$ limit, we can distinguish whether T_{RW} decreases or increases. For example in Ref. [27, 2], we can see that Eq. (3) is negative below T_{RW} and it becomes moderate above T_{RW} . The μ_R^2 correction term makes $\text{Re } \mathcal{V}$ with $C_{-\epsilon}$ higher than that with $C_{+\epsilon}$ because the μ_R^2 correction term is then positive with $C_{+\epsilon}$. This means that T_{RW} decreases with increasing μ_R at least in

the small μ_R region. This behavior is consistent with the decreasing behavior of the pseudo-critical temperature of deconfinement transition defined by using usual determinations; for example, see Refs [17, 28, 29].

5. QCD phase diagram at complex chemical potential

By taking into account our perturbative result and the symmetry argument, we can sketch expected QCD phase diagrams at finite complex chemical potential. Phase diagrams expected from our present discussions are summarized in Fig. 2. Because

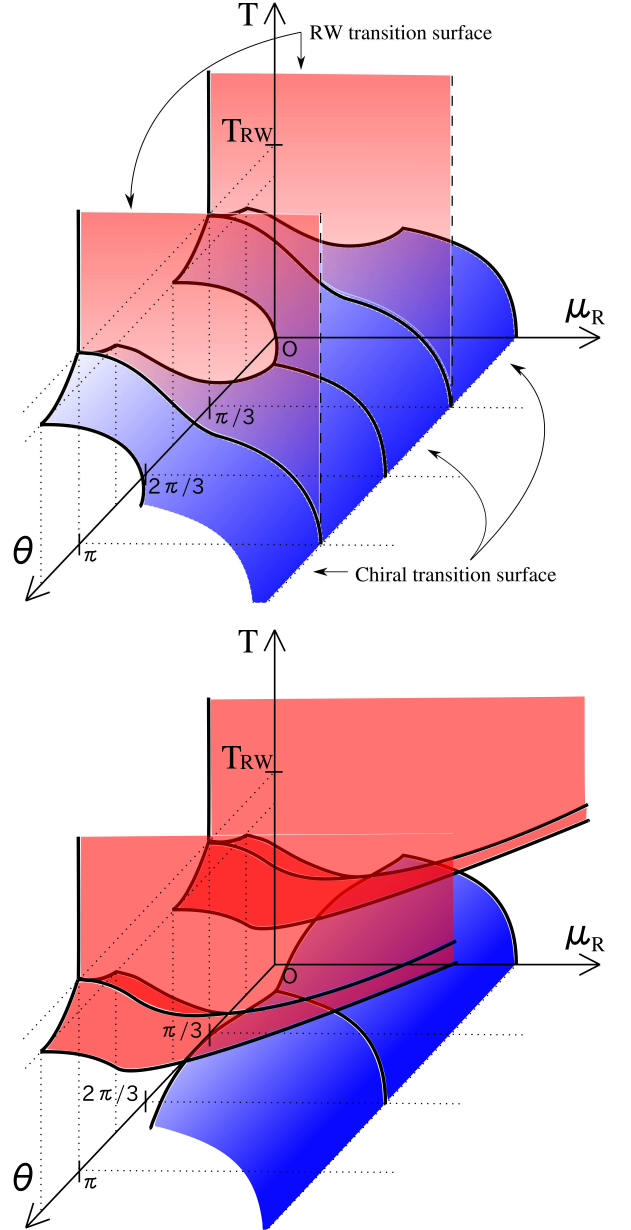


Figure 2: Two possible schematic QCD phase diagrams at finite complex chemical potential. The top (bottom) panel represents the correlated (uncorrelated) case between the chiral and RW transition surfaces.

of the RW periodicity, the phase structure should be periodic along the θ axis.

The RW transition line on the (T, θ) plane ($\mu_R = 0$) may be topologically connected with the first order phase transition boundary on the (T, μ_R) plane ($\theta = 0$). Two of the first order transition lines starting from the RW endpoint have chiral transition nature and are referred to as the *chiral transition lines* [7]. Then it is not unreasonable to expect that the endpoint of the chiral critical line on the (T, θ) plane is connected with the QCD critical point on the (T, μ_R) plane. In this case, the first order phase boundary on the (T, μ_R) plane forms a chiral transition surface in the (T, μ_R, θ) space, and connects the (T, μ_R) plane and the (T, θ) plane. The RW transition line extends in the finite μ_R region and forms an RW transition surface in the (T, μ_R, θ) space. The RW endpoint may reach $T = 0$ as shown in the top panel of Fig. 2 or it may deviate from the chiral transition surface at some temperature. There is the possibility that T_{RW} line becomes smaller than the chiral critical surface at moderate μ_R and finally becomes larger than the chiral transition surface.. It is deeply related with a strength of the correlation between the chiral transition surface and the RW transition surface.

Another possibility is that the first order transition lines on the (T, θ) plane are topologically separated from the first order phase boundary on the (T, μ_R) plane, as shown in the bottom panel of Fig. 2. T_{RW} first decreases at small μ_R , but does not go across the chiral transition surface. In this case, the deconfinement transition represented by the RW transition line on the (T, θ) plane has less relevance to the first order phase boundary, which would be the chiral transition, on the (T, μ_R) plane. Therefore, we can call this possibility *uncorrelated case* and the former possibility *correlated case*.

The QCD phase diagram at finite complex chemical potential is related with the following subjects. (I) In Ref. [30, 31], the authors use experimental data to construct the canonical partition function. Then, T_{RW} at $\mu_R = 0$ is used to clarify realized temperatures in experiments through the Lee-Yang zero analysis [32, 33]. In the analysis, T_{RW} at finite μ_R should be related with zeros inside the unit circle on the complex quark fugacity plane. If so, there is the possibility that we can strictly determine realized temperatures in experiments if we can systematically understand the behavior of zeros. (II) The analytic continuation in QCD from the imaginary to the real chemical potential is usually performed on the μ^2 plane. In the continuation, we may miss some information such as an inhomogeneous condensate [34]. The analytic continuation on the complex chemical potential plane may restore the information missing.

6. Summary

We proposed the new definition of the pseudo-critical temperature of the deconfinement transition by considering the imaginary chemical potential. The imaginary chemical potential can be interpreted as the Aharonov-Bohm phase induced by $U(1)$ flux insertions and then the analogy of the topological order can be used. In the deconfined phase, we can find the degeneracy of the free energy by inserting the $U(1)$ flux, and these

states belong to different minima. On the other hand, in the confined phase, we cannot find such non-trivial structure of the free energy. This suggests that we can distinguish the confined and deconfined phases at $\theta = \mu_1/T = 0$ from the non-trivial degeneracy of the effective potential at $\theta = \pi/N_c$. Then, T_{RW} becomes the pseudo-critical temperature at $\mu = 0$.

Using the perturbative expansion in terms of μ_R , we investigated the behavior of T_{RW} at small μ_R and then the decreasing behavior of T_{RW} was obtained. Based on these results, we presented two scenarios of the QCD phase diagram at finite complex chemical potential. First scenario which is the correlated case has the strong correlation between the chiral and deconfinement transitions. The RW endpoint at finite μ_R finally reaches the $T = 0$ point. Then, the critical point can become more complex than the usual expectation since two more first order transition lines can be connected at the critical point. The second scenario is the uncorrelated case. The RW endpoint is separated from the chiral transition surface.

Since the complex chemical potential is related with the Lee-Yang zero analysis and the analytic continuation to the finite μ_R region, understanding the QCD phase structure at finite complex chemical potential may have impact to the beam energy scan program in heavy ion collider experiments, investigation of neutron star structures and so on. Our results are based on perturbative calculations and thus the non-perturbative checks should be done.

K.K. thanks Hiroaki Kouno, Keitaro Nagata and Masanobu Yahiro for useful discussions and comments. He is especially thankful to Yoshimasa Hidaka for his comment which motivates us to start this study. K.K. is supported by Grants-in-Aid for Japan Society for the Promotion of Science (JSPS) fellows (No.26-1717). A.O. is supported in part by KAKENHI (Nos. 23340067, 24340054, 24540271, 15K05079, 24105001, 24105008), and by the Yukawa International Program for Quark-Hadron Sciences.

References

- [1] P. de Forcrand, Simulating QCD at finite density, PoS LAT2009 (2009) 010. arXiv:1005.0539.
- [2] Y. Sakai, K. Kashiwa, H. Kouno, M. Yahiro, Phase diagram in the imaginary chemical potential region and extended $Z(3)$ symmetry, Phys.Rev. D78 (2008) 036001. arXiv:0803.1902, doi:10.1103/PhysRevD.78.036001.
- [3] K. Kashiwa, M. Matsuzaki, H. Kouno, Y. Sakai, M. Yahiro, Meson mass at real and imaginary chemical potentials, Phys.Rev. D79 (2009) 076008. arXiv:0812.4747, doi:10.1103/PhysRevD.79.076008.
- [4] A. Roberge, N. Weiss, Gauge Theories With Imaginary Chemical Potential and the Phases of QCD, Nucl.Phys. B275 (1986) 734. doi:10.1016/0550-3213(86)90582-1.
- [5] X. Wen, Topological Order in Rigid States, Int.J.Mod.Phys. B4 (1990) 239. doi:10.1142/S0217979290000139.
- [6] M. Sato, Topological discrete algebra, ground state degeneracy, and quark confinement in QCD, Phys.Rev. D77 (2008) 045013. arXiv:0705.2476, doi:10.1103/PhysRevD.77.045013.
- [7] M. D'Elia, F. Sanfilippo, The Order of the Roberge-Weiss endpoint (finite size transition) in QCD, Phys.Rev. D80 (2009) 111501. arXiv:0909.0254, doi:10.1103/PhysRevD.80.111501.
- [8] C. Bonati, G. Cossu, M. D'Elia, F. Sanfilippo, The Roberge-Weiss endpoint in $N_f = 2$ QCD, Phys.Rev. D83 (2011) 054505. arXiv:1011.4515, doi:10.1103/PhysRevD.83.054505.

- [9] C. Bonati, P. de Forcrand, M. D’Elia, O. Philipsen, F. Sanfilippo, Chiral phase transition in two-flavor QCD from an imaginary chemical potential, *Phys.Rev. D90* (7) (2014) 074030. [arXiv:1408.5086](#), [doi:10.1103/PhysRevD.90.074030](#).
- [10] Y. Nishida, Phase structures of strong coupling lattice QCD with finite baryon and isospin density, *Phys.Rev. D69* (2004) 094501. [arXiv:hep-ph/0312371](#), [doi:10.1103/PhysRevD.69.094501](#).
- [11] N. Kawamoto, K. Miura, A. Ohnishi, T. Ohnuma, Phase diagram at finite temperature and quark density in the strong coupling limit of lattice QCD for color SU(3), *Phys.Rev. D75* (2007) 014502. [arXiv:hep-lat/0512023](#), [doi:10.1103/PhysRevD.75.014502](#).
- [12] R. Garcia Martin, J. Pelaez, Chiral condensate thermal evolution at finite baryon chemical potential within Chiral Perturbation Theory, *Phys.Rev. D74* (2006) 096003. [arXiv:hep-ph/0608320](#), [doi:10.1103/PhysRevD.74.096003](#).
- [13] A. Ayala, A. Bashir, C. Dominguez, E. Gutierrez, M. Loewe, et al., QCD phase diagram from finite energy sum rules, *Phys.Rev. D84* (2011) 056004. [arXiv:1106.5155](#), [doi:10.1103/PhysRevD.84.056004](#).
- [14] D. J. Gross, R. D. Pisarski, L. G. Yaffe, QCD and Instantons at Finite Temperature, *Rev.Mod.Phys.* 53 (1981) 43. [doi:10.1103/RevModPhys.53.43](#).
- [15] N. Weiss, The Effective Potential for the Order Parameter of Gauge Theories at Finite Temperature, *Phys.Rev. D24* (1981) 475. [doi:10.1103/PhysRevD.24.475](#).
- [16] Y. Aharonov, D. Bohm, Significance of electromagnetic potentials in the quantum theory, *Phys.Rev.* 115 (1959) 485–491. [doi:10.1103/PhysRev.115.485](#).
- [17] K. Fukushima, Chiral effective model with the Polyakov loop, *Phys.Lett. B591* (2004) 277–284. [arXiv:hep-ph/0310121](#), [doi:10.1016/j.physletb.2004.04.027](#).
- [18] K. Fukushima, Y. Hidaka, A Model study of the sign problem in the mean-field approximation, *Phys.Rev. D75* (2007) 036002. [arXiv:hep-ph/0610323](#), [doi:10.1103/PhysRevD.75.036002](#).
- [19] H. Nishimura, M. C. Ogilvie, K. Pangaeni, Complex saddle points in QCD at finite temperature and density [arXiv:1401.7982](#).
- [20] H. Nishimura, M. C. Ogilvie, K. Pangaeni, Complex Saddle Points and Disorder Lines in QCD at finite temperature and density [arXiv:1411.4959](#).
- [21] Y. Tanizaki, H. Nishimura, K. Kashiwa, Evading the sign problem in the mean-field approximation through Lefschetz-thimble path integral [arXiv:1504.02979](#).
- [22] E. Witten, Analytic Continuation Of Chern-Simons Theory (2010) 347–446 [arXiv:1001.2933](#).
- [23] M. Cristoforetti, F. Di Renzo, L. Scorzato, New approach to the sign problem in quantum field theories: High density QCD on a Lefschetz thimble, *Phys.Rev. D86* (2012) 074506. [arXiv:1205.3996](#), [doi:10.1103/PhysRevD.86.074506](#).
- [24] H. Fujii, D. Honda, M. Kato, Y. Kikukawa, S. Komatsu, et al., Hybrid Monte Carlo on Lefschetz thimbles - A study of the residual sign problem, *JHEP* 1310 (2013) 147. [arXiv:1309.4371](#), [doi:10.1007/JHEP10\(2013\)147](#).
- [25] G. Parisi, Y.-s. Wu, Perturbation Theory Without Gauge Fixing, *Sci.Sin.* 24 (1981) 483.
- [26] G. Parisi, ON COMPLEX PROBABILITIES, *Phys.Lett. B131* (1983) 393–395. [doi:10.1016/0370-2693\(83\)90525-7](#).
- [27] M. D’Elia, M.-P. Lombardo, Finite density QCD via imaginary chemical potential, *Phys.Rev. D67* (2003) 014505. [arXiv:hep-lat/0209146](#), [doi:10.1103/PhysRevD.67.014505](#).
- [28] C. Sasaki, B. Friman, K. Redlich, Susceptibilities and the Phase Structure of a Chiral Model with Polyakov Loops, *Phys.Rev. D75* (2007) 074013. [arXiv:hep-ph/0611147](#), [doi:10.1103/PhysRevD.75.074013](#).
- [29] K. Kashiwa, H. Kouno, M. Matsuzaki, M. Yahiro, Critical endpoint in the Polyakov-loop extended NJL model, *Phys.Lett. B662* (2008) 26–32. [arXiv:0710.2180](#), [doi:10.1016/j.physletb.2008.01.075](#).
- [30] A. Nakamura, K. Nagata, Probing QCD Phase Structure by Baryon Multiplicity Distribution [arXiv:1305.0760](#).
- [31] K. Nagata, K. Kashiwa, A. Nakamura, S. M. Nishigaki, Lee-Yang zero distribution of high temperature QCD and Roberge-Weiss phase transition [arXiv:1410.0783](#).
- [32] C.-N. Yang, T. Lee, Statistical theory of equations of state and phase transitions. 1. Theory of condensation, *Phys.Rev.* 87 (1952) 404–409. [doi:10.1103/PhysRev.87.404](#).
- [33] T. Lee, C.-N. Yang, Statistical theory of equations of state and phase transitions. 2. Lattice gas and Ising model, *Phys.Rev.* 87 (1952) 410–419. [doi:10.1103/PhysRev.87.410](#).
- [34] K. Kashiwa, T. Lee, K. Nishiyama, Y. Yoshiike, in progress.